2009 American Control Conference
Hyatt Regency Riverfront, St. Louis, MO, USA
June 10-12, 2009

Leader-Follower Dynamics for Unicycles

Siming Zhao, Abhishek Halder, Tamás Kalmár-Nagy

Abstract— **This paper analyzes the leader-follower dynamics for nonholonomic vehicle (unicycle). Local stability of the system is studied in global and local coordinates. The bifurcation structure of the system is studied and we demonstrate the existence of Hopf and Fold-Hopf bifurcations in the system depending on the choice of control gain.**

I. Introduction

In recent years, multi-agent systems have become a ubiquitous area of research across disciplines like biology ([1], [2], [3]), computer graphics [4] and systems science and engineering. Owing to its varied application domains in systems and control research ([5], [6], [7], [8]), various facets of multi-agent systems have been explored including modeling, stability and control. The prime motivation of the research endeavor has been to achieve desired formations of the agent collectives. *Consensus seeking* [9] or the *state agreement problem* [10] deals with designing feedback control laws to make multiple agents converge to a global configuration. A special case to this is the *rendezvous problem* ([11], [12]) where the agents converge at a single location.

Starting from the *n*-bug problem in mathematics [13], the self-propelled planar particles were later replaced by wheeled mobile agents with single nonholonomic constraint i.e. unicycles ([14], [15]). Several researchers ([14], [15], [16], [17], [18]) proposed control laws for such nonholonomic vehicles. One possible approach to design the control law is to use a centralized cooperative control scheme for the entire agent collective. However, such a law is susceptible to bandwidth limitation as well as external disturbances and hence not scalable for a team having large number of mobile agents. As a result, distributed control laws have been investigated by the researchers for this problem, where the feedback is constructed through local interactions of the vehicles leading to a global formation convergence. In particular, Yang *et al.* [19] proposed a decentralized framework where a distributed controller accounts for local control decision based on the interaction of each agent with its neighbors. A special research topic has been to design the distributed controller with asynchronous communication constraints. For a detailed account on this topic, the reader may refer to ([21], [22], [23], [24]). A bio-inspired optimal co-operative control strategy was implemented in [25] for leader-follower pursuit problem.

The present paper is part of a research endeavor which aims to address the nonholonomic multi-agent dynamics and distributed control problem with communication delay. Before addressing the general n-nonholonomic agent problem, the authors aim to assess the 2 unicycle problem with delay. As a simplifying case to that, the authors studied the cyclic pursuit of 2-nonholonomic agent problem without communication delay [27] with a controller similar to [14] but modified to avoid the orientation singularity. These preliminary results showed that the system may exhibit very different dynamics depending on the choice of controller gains and such regimes were calculated. As a next step, in this paper, the authors present nonlinear dynamics of two nonholonomic vehicles in leader-follower configuration to characterize similar regimes and system parameter dependence which, the authors believe, throws light in many nontrivial areas of the complex dynamics of the agents leading to greater understanding of the overall system. In this paper, the local stability analysis has been performed and numerical results are presented to illustrate the dynamics of the agent collective.

As mentioned above, the choice of leader-follower configuration was partly due to its slightly simpler dynamics and partly due to the fact that many biological systems (like birds) also exhibit this configuration. This choice in the biological world was long believed to be for energy efficiency [29]. Some recent results [30] tell that leader-follower configuration may also enhance communication and orientation of the flock. It is a topic of research whether this form may have any superiority in inter-agent communication and performance for the bio-mimetic collectives.

The rest of this paper is organized as follows. Section II describes the mathematical model considered in this paper and transforms the equations of motion from global coordinates to relative coordinates. Section III provide the fixed points of the system and provide the trajectories in the global coordinates. Section IV begins with the calculation of stability boundary and then bifurcation structure of the dynamics is described in detail. The existence of Hopf bifurcation and fold-Hopf bifurcation, depending on the value of scaled control gain, are shown and simulation results are presented. Section VI summarizes the results of this paper and indicates current research directions.

II. Model description

The focus of this paper is to investigate the dynamics of two unicycles where the trajectory of the leader is characterized by constant linear and angular velocities (V and ω)

$$\begin{aligned} v_1 &= V, \\ \omega_1 &= \omega. \end{aligned} \tag{1}$$

S. M. Zhao, A. Halder and T. Kalmár-Nagy are with the Department of Aerospace Engineering, Texas A&M University, College Station, Texas, 77843, USA. {s0z0239, a0h7710}@aeromail.tamu.edu, acc2009@kalmarnagy.com

The case $\omega = 0$ represents straight line motion, while $\omega \neq 0$ corresponds to circular motion. The position and orientation of the i^{th} vehicle ($i = 1$ for the leader and $i = 2$ for the follower) are denoted by $(x_i, y_i)^T \in \mathbb{R}^2$ and $\theta_i \in [-\pi, \pi)$, respectively. The kinematic equations for the follower are

$$\begin{pmatrix} \dot{x}_2(t) \\ \dot{y}_2(t) \\ \dot{\theta}_2(t) \end{pmatrix} = \begin{pmatrix} \cos\theta_2(t) & 0 \\ \sin\theta_2(t) & 0 \\ 0 & 1 \end{pmatrix} \begin{pmatrix} \upsilon_2 \\ \omega_2 \end{pmatrix}, \qquad (2)$$

where $(\upsilon_2, \omega_2)^T \in \mathbb{R}^2$ are control inputs (velocity and angular velocity).

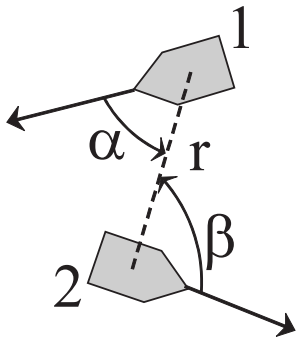

Fig. 1. Relative coordinates with vehicle 2 pursuing vehicle 1

The configuration of two unicycles is shown in Fig. 1, where r is the relative distance between the two vehicles, α is the angle between the current orientation of vehicle 1 and the line of sight, and β is the angle between the current orientation of vehicle 2 and the line of sight. Both angles are positive in the sense of counterclockwise rotation to the line of sight. Following [14], the kinematic equations are written in relative coordinates:

$$\begin{aligned} \dot{r} &= -\upsilon_1 \cos\alpha - \upsilon_2 \cos\beta, \\ \dot{\alpha} &= \frac{1}{r}(\upsilon_1 \sin\alpha + \upsilon_2 \sin\beta) - \omega_1, \\ \dot{\beta} &= \frac{1}{r}(\upsilon_1 \sin\alpha + \upsilon_2 \sin\beta) - \omega_2. \end{aligned} \qquad (3)$$

where $r \in \mathbb{R}^+$ and $(\alpha, \beta) \in \mathscr{S}^2$. The pursuit control law is chosen as

$$\begin{aligned} \upsilon_2 &= r, \\ \omega_2 &= k \sin\beta, \end{aligned} \qquad (4)$$

where the gain k is positive. Substituting the control law into the relative dynamics (3) yields

$$\begin{aligned} \dot{r} &= -V\cos\alpha - r\cos\beta, \\ \dot{\alpha} &= \frac{1}{r}(V\sin\alpha + r\sin\beta) - \omega, \\ \dot{\beta} &= \frac{1}{r}(V\sin\alpha + r\sin\beta) - k\sin\beta. \end{aligned} \qquad (5)$$

The parameters of this system are V, ω and k and are restricted to be positive.

III. Characterization of equilibria

A. Fixed points of the system

Setting the right hand side of (5) to zero results three transcendental equations for the fixed points of the system

$$\frac{V}{r^*}\cos\alpha^* = -\cos\beta^*, \qquad (6)$$

$$\frac{V}{r^*}\sin\alpha^* = -\sin\beta^* + \omega, \qquad (7)$$

$$\frac{V}{r^*}\sin\alpha^* = (k-1)\sin\beta^*. \qquad (8)$$

Subtracting (7) from (8) yields

$$\sin\beta^* = \frac{\omega}{k}. \qquad (9)$$

Fixed point(s) exist when $|\sin\beta^*| \leqslant 1$, i.e. $k \geqslant \omega$. When $k = \omega$, two fixed points coalesce in a saddle-node bifurcation.

Squaring and adding (6) and (7) yields

$$(\frac{V}{r^*})^2 = 1 + \omega^2 - \frac{2\omega^2}{k},$$

which results the equilibrium relative distance as

$$r^* = \frac{V}{\sqrt{1+\omega^2-\frac{2\omega^2}{k}}}, \quad 1+\omega^2-\frac{2\omega^2}{k} > 0. \qquad (10)$$

Further, substituting (9) and (10) into (7) yields

$$\sin\alpha^* = \frac{\omega - \frac{\omega}{k}}{\sqrt{1+\omega^2-\frac{2\omega^2}{k}}}. \qquad (11)$$

From (6), it can be noted that $\cos\alpha^*$ and $\cos\beta^*$ must have different signs.

When $k > \omega$, the two fixed points are $A(r^*, \alpha_A^*, \beta_A^*)$ and $B(r^*, \alpha_B^*, \beta_B^*)$ with

$$\begin{aligned} \alpha_A^* &= \pi - \arcsin\omega\frac{k-1}{k\sqrt{1+\omega^2-\frac{2\omega^2}{k}}}, \quad \beta_A^* = \arcsin\frac{\omega}{k}, \\ \alpha_B^* &= \arcsin\omega\frac{k-1}{k\sqrt{1+\omega^2-\frac{2\omega^2}{k}}}, \quad \beta_B^* = \pi - \arcsin\frac{\omega}{k}. \end{aligned} \qquad (12)$$

When $k = \omega \neq 1$, there is only one fixed point (as noted above) and is given by $(r^*, \alpha^*, \beta^*) = (\frac{V}{|1-k|}, \frac{\pi}{2}, \frac{\pi}{2})$.

B. Equilibrium formations in global coordinates

Fixed points A and B correspond to equilibrium formations in global coordinates (x, y, θ). The goal of this section is to characterize these formations, as these correspond to the physical behavior of the system. When $\omega = 0$, the trajectory of the leader can be expressed explicitly as

$$\begin{aligned} x_1(t) &= (V\cos\theta_0)t + x_0, \\ y_1(t) &= (V\sin\theta_0)t + y_0, \\ \theta_1 &= \theta_0, \end{aligned} \qquad (13)$$

where (x_0, y_0, θ_0) are the initial positions and orientation of the leader. It is straightforward to observe that fixed point $A(V, 0, 0)$ corresponds to the rectilinear motion of the

follower. When $\omega \neq 0$, the trajectory of the leader (c.f. (1)) can be expressed explicitly as

$$\begin{aligned} x_1(t) &= \frac{V}{\omega}\sin(\omega t+\theta_0)+x_c, \\ y_1(t) &= -\frac{V}{\omega}\cos(\omega t+\theta_0)+y_c, \\ \theta_1 &= \omega t+\theta_0, \end{aligned} \tag{14}$$

where θ_0 is initial orientation of the leader, $x_c = x_1(0) - \frac{V_c}{\omega}\sin\theta$ and $y_c = y_1(0)+\frac{V_c}{\omega}\cos\theta$ are the center of the circle of radius $R_1 = \frac{V}{\omega}$ describing the locus of the leader. Without loss of generality, one can choose $x_c = y_c = 0$.

Representing the fixed point equations (10) and (12) in global coordinates finally yields the the locus of the follower

$$x_2^2+y_2^2 = \frac{V^2}{\omega^2}\frac{1}{1+\omega^2-\frac{2\omega^2}{k}} = R_2^2. \tag{15}$$

Thus in the equilibrium formation, the follower is circling the origin with radius R_2. Figures 2 show the "pursuit graph" (parametric plots of $\{x_i(t), y_i(t)\}$) for circular ($\omega > 0$) and straight line ($\omega = 0$) leader-follower trajectories, respectively.

IV. Local stability analysis

The local stability of the fixed points is determined by the eigenstructure of the Jacobian evaluated at the fixed point. The Jacobian of (5) is given by

$$\mathscr{J}_p = \begin{pmatrix} -\cos\beta^* & V\sin\alpha^* & r^*\sin\beta^* \\ -\frac{V}{r^{*2}}\sin\alpha^* & \frac{V}{r^*}\cos\alpha^* & \cos\beta^* \\ -\frac{V}{r^{*2}}\sin\alpha^* & \frac{V}{r^*}\cos\alpha^* & (1-k)\cos\beta^* \end{pmatrix}. \tag{16}$$

The characteristic polynomial of the Jacobian, evaluated at the fixed points A and B, is given by ($+$ and $-$ corresponds to A and B, resp.):

$$\lambda^3 \pm p_2\lambda^2 + p_1\lambda \pm p_0 = 0, \tag{17}$$

where $p_2 = (1+\frac{1}{k})\sqrt{k^2-\omega^2}$, $p_1 = \omega^2+2k-\frac{3\omega^2}{k}$ and $p_0 = (1+\omega^2-\frac{2\omega^2}{k})\sqrt{k^2-\omega^2}$. The characteristic equation corresponding to fixed point B can be obtained from that of fixed point A by the transformation $\lambda \to -\lambda$, so the spectrum of B is the reflection of that of A about the imaginary axis.

A. Stability criteria

A fixed point is stable when the corresponding characteristic polynomial is Hurwitz. Applying necessary and sufficient condition on Hurwitz stability of a third order polynomial [31] results

$$2k^3+k^2-3\omega^2 > 0, \tag{18}$$

$$1+\omega^2-\frac{2\omega^2}{k} > 0. \tag{19}$$

From (9), the existence of the fixed points requires

$$k \geqslant \omega. \tag{20}$$

Inequalities (18), (19) and (20) determine regions in the $k-\omega$ parameter space where fixed points exists, as well as their stability. These regions are characterized by the three curves

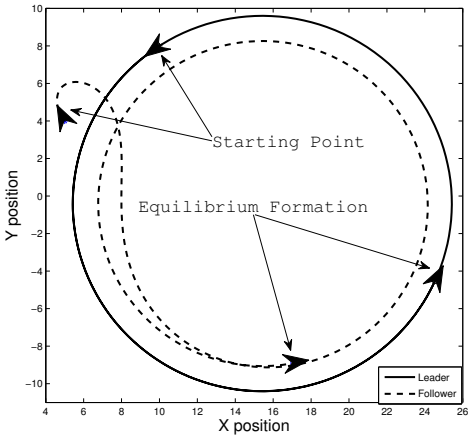

(a) $\omega \neq 0$

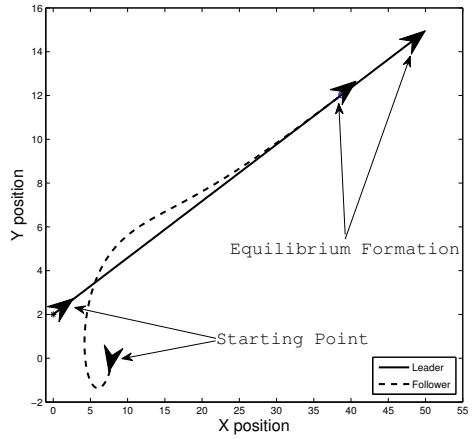

(b) $\omega = 0$

Fig. 2. Circular and Straight line motion pursuit graph in global coordinate

$\omega_1(k) = k$, $\omega_2(k) = \sqrt{\frac{2k^3+k^2}{3}}$ and $\omega_3(k) = \sqrt{\frac{k}{2-k}}$ $(k < 2)$. Notice that when $k \geqslant 2$, inequality (19) is alway satisfied, the stability region is determined only by the remaining two curves. It can be easily verified that $\omega_1(k) \leqslant \omega_3(k)$ when $0 < k < 2$. Fig. 3 depicts the stability boundaries of this system. It can be observed that when $\omega = 0$ (straight line motion), fixed point $A = (V, \pi, 0)$ is always a stable node while $B = (V, 0, \pi)$ is always an unstable one.

V. Hopf bifurcation

When $0 < k < 1$, the characteristic polynomial on the curve $\omega_2(k)$ can be written as

$$\big(\lambda+(1+\frac{1}{k})\sqrt{k^2-\omega^2}\big)(\lambda^2+\omega^2+2k-\frac{3\omega^2}{k}) = 0.$$

This implies that for the fixed point A, the Jacobian has one negative real eigenvalue and a pair of complex conjugate on the imaginary axis. Below the curve $\omega_2(k)$, the Jacobian has one negative real eigenvalue and a pair of complex

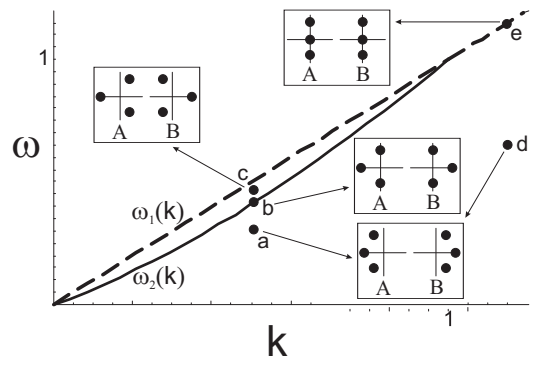

Fig. 3. Linear stability boundary for system (5) with spectra of A and B

conjugate on the left half plane, i.e. stable node-focus. Between the curve $\omega_2(k)$ and $\omega_1(k)$, the pair of complex conjugate eigenvalues have positive real part, which suggests the occurrence of Hopf bifurcation by increasing k through $\omega_2(k)$. On this curve, the critical bifurcation value of ω is $\omega_c = \sqrt{\frac{2k^3+k^2}{3}}$, and the root crossing velocity can be calculated as

$$\mathrm{Re}\frac{d\lambda}{d\omega}|_{(k,\omega_c)} = \frac{3\sqrt{2}}{7k+2}\sqrt{\frac{1+2k}{1-k}} > 0. \qquad (21)$$

This establishes a necessary condition for the Hopf bifurcation. To show that the fixed point of the dynamical system (5) is weakly attracting/repelling on the stability boundary, one needs to compute the so-called Poincaré-Lyapunov constant [33]. To find this constant, the original equation (5) is expanded up to third order around fixed point A [32]

$$\dot{\mathbf{w}} = \blacksquare(\mathbf{w}) = \mathscr{J}_p\mathbf{w} + \frac{1}{2}\mathbf{f}^{(2)}(\mathbf{w}) + \frac{1}{6}\mathbf{f}^{(3)}(\mathbf{w}) + \mathscr{O}(\mathbf{w}^4), \quad (22)$$

where $\mathbf{w} = (r - r_A^*, \alpha - \alpha_A^*, \beta - \beta_A^*)^T$ defines new coordinates which shift the fixed point A to the origin. In these new coordinates, $\mathbf{f}^{(2)}(\mathbf{w})$ and $\mathbf{f}^{(3)}(\mathbf{w})$ are multilinear vector functions given by

$$\mathbf{f}_i^{(2)} = \sum_{j,k=1}^{n} \frac{\partial^2 \blacksquare_i(\xi)}{\partial\xi_j\partial\xi_k}|_{\xi=0}\mathbf{w}_j\mathbf{w}_k \qquad i = 1,2,3,$$

and

$$\mathbf{f}_i^{(3)} = \sum_{j,k,l=1}^{n} \frac{\partial^3 \blacksquare_i(\xi)}{\partial\xi_j\partial\xi_k\partial\xi_l}|_{\xi=0}\mathbf{w}_j\mathbf{w}_k\mathbf{w}_l \qquad i = 1,2,3.$$

In order to obtain the real Jordan canonical form, a linear transformation $\mathbf{T}$ needs to be constructed using the eigenvectors of the Jacobian evaluated at ω_c. At the critical point, the pair of complex conjugate eigenvalues have the form $\lambda_{2,3} = \pm i\omega_0$,

$$\omega_0 = \sqrt{k(1-\frac{2}{3}k)(1-k)} > 0.$$

Let $\mathbf{q}_2 \in \mathscr{C}^3$ be the complex eigenvector corresponding to the eigenvalue λ_2. Then,

$$\mathscr{J}_p\mathbf{q}_2 = i\omega_0\mathbf{q}_2, \quad \mathscr{J}_p\bar{\mathbf{q}}_2 = -i\omega_0\bar{\mathbf{q}}_2$$

Also, let $\mathbf{q}_1 \in \mathscr{R}^3$ be the real eigenvector corresponding to the eigenvalue $\lambda_1 = -(1+k)\sqrt{\frac{2}{3}(1-k)}$, i.e. $\mathscr{J}_p\mathbf{q}_1 = \lambda_1\mathbf{q}_1$. The transformation matrix $\mathbf{T}$ is composed by $\frac{1}{\|\mathbf{q}_1\|}(\mathrm{Re}\mathbf{q}_2, -\mathrm{Im}\mathbf{q}_2, \|\mathbf{q}_1\|\mathbf{q}_1)$ where $\mathbf{q}_1$ and $\mathbf{q}_2$ are given by

$$\mathbf{q}_2 = \begin{pmatrix} \frac{2\sqrt{6}Vk}{9\gamma\sqrt{1-k}} + i\frac{Vk(1-\frac{2}{3}k)}{3\omega_0\gamma} \\ 1 \\ 1-\frac{2}{3}k + i\frac{\sqrt{6}\omega_0}{3\sqrt{1-k}} \end{pmatrix}, \mathbf{q}_1 = \begin{pmatrix} -\frac{\sqrt{6}V(1+2k)}{3\gamma\sqrt{1-k}} \\ 1 \\ k+1 \end{pmatrix}$$
$$\gamma = \frac{1}{3}\sqrt{(3-2k)(1+2k)(1-k^2)}.$$

Introducing the transformation $\mathbf{y} = \mathbf{T}^{-1}\mathbf{w}$

$$\dot{\mathbf{y}} = \mathbf{J}\mathbf{y} + \frac{1}{2}\mathbf{g}^{(2)}(\mathbf{y}) + \frac{1}{6}\mathbf{g}^{(3)}(\mathbf{y}) + \mathscr{O}(\mathbf{y}^4), \qquad (23)$$

where the Jordan canonical form $\mathbf{J}$ is given by

$$\mathbf{J} = \mathbf{T}^{-1}\mathscr{J}_p\mathbf{T} = \begin{pmatrix} 0 & -\omega_0 & 0 \\ \omega_0 & 0 & 0 \\ 0 & 0 & \lambda_1 \end{pmatrix}.$$

In (23), the nonlinear vector functions in transformed coordinates are given by

$$\mathbf{g}^{(2)}(\mathbf{y}) = \mathbf{T}^{-1}\mathbf{f}^{(2)}(\mathbf{w})|_{\mathbf{w}=\mathbf{T}\mathbf{y}},$$
$$\mathbf{g}^{(3)}(\mathbf{y}) = \mathbf{T}^{-1}\mathbf{f}^{(3)}(\mathbf{w})|_{\mathbf{w}=\mathbf{T}\mathbf{y}}.$$

Assuming that the center manifold has the quadratic form $y_3 = \frac{1}{2}(h_1y_1^2 + 2h_2y_1y_2 + h_3y_2^2)$, one can reduce (23) into a two-dimensional system up to third order

$$\begin{aligned} \dot{y}_1 &= -\omega_0 y_2 + a_{20}y_1^2 + a_{11}y_1y_2 + a_{02}y_2^2 \\ &\quad + a_{30}y_1^3 + a_{21}y_1^2y_2 + a_{12}y_1y_2^2 + a_{03}y_2^3, \\ \dot{y}_2 &= \omega_0 y_1 + b_{20}y_1^2 + b_{11}y_1y_2 + b_{02}y_2^2 \\ &\quad + b_{30}y_1^3 + b_{21}y_1^2y_2 + b_{12}y_1y_2^2 + b_{03}y_2^3. \end{aligned} \qquad (24)$$

From the above normal form, the direction of the Hopf bifurcation can be determined from the so-called Poincaré-Lyapunov constant [33].

VI. Numerical Results

A. Hopf bifurcation

Fig. 4 shows the phase portrait corresponding to point a on the stability chart (Fig. 3) and the associated pursuit graph. Fixed point A is exponentially attracting here. Fig. 5 depicts the phase portrait associated with point b showing a weakly attracting fixed point A. There is a stable limit cycle born (supercritical Hopf bifurcation) around the fixed point A (point c) when ω is increased through its critical value ω_c (phase portrait and pursuit graph are shown in Fig. 6). The pursuit trajectory in global coordinates has two harmonic components.

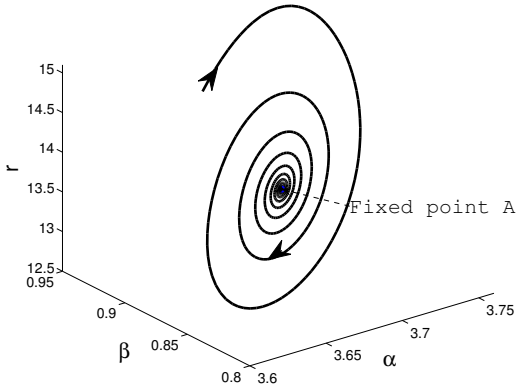

(a) Phase portrait at point *a*

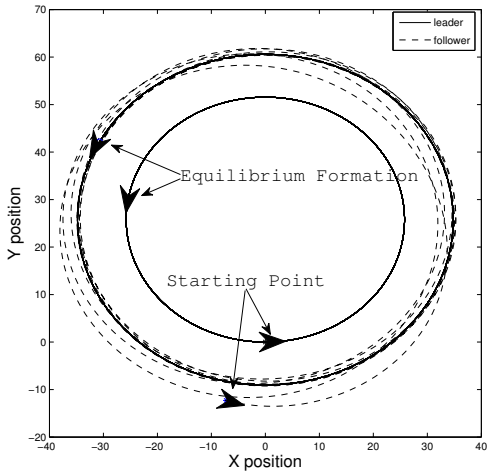

(b) Pursuit graph for point *a* in global coordinates

Fig. 4. Phase portrait at point *a* when fixed point *A* is attracting and the corresponding pursuit graph in global coordinates

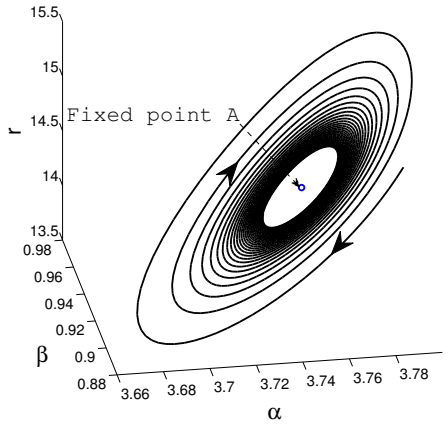

Fig. 5. Phase portrait at point *b* where the fixed point *A* is a weakly attracting one

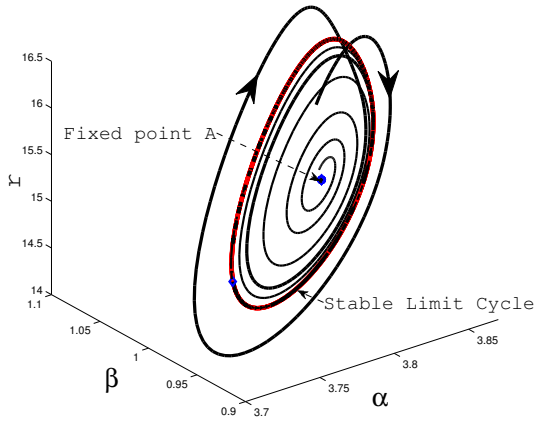

(a) Phase portrait at point *c*

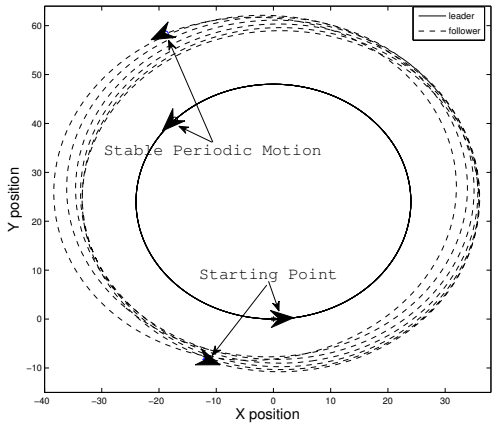

(b) Pursuit graph in global coordinates

Fig. 6. Phase portrait at point *c* when a stable limit cycle is born near fixed point *A* and the corresponding pursuit graph

B. Fold-Hopf bifurcation

When $k > 1$, the characteristic polynomial on the stability curve $\omega_1(k)$ can be written as

$$\lambda^3 + (\omega^2 - \omega)\lambda = 0$$

implying that there is zero eigenvalue together with a pair of pure imaginary ones. This is a Fold-Hopf (a codimension-two) bifurcation [33]. Fig. 7.a shows the phase portrait of a point situated slightly below the point *e* on the stability curve $k = \omega$. Fig. 7.b shows the pursuit graph on the point *e*, due to the complexity of Fold-Hopf bifurcation, what exactly happens in this case needs further investigation.

VII. Conclusions

In this paper, leader-follower pursuit is introduced for unicycles. Local stability analysis around the equilibrium formation has been performed. Analysis and numerical simulations have shown the existence of Hopf and Fold-Hopf

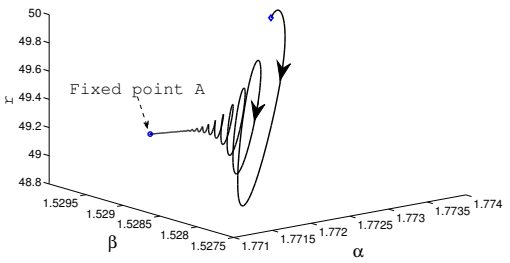

(a) Phase portrait slightly below point *e*

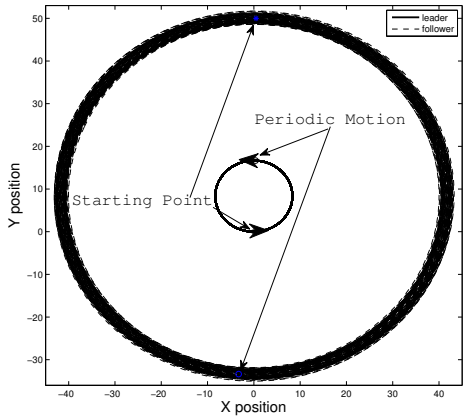

(b) Pursuit graph in global coordinates

Fig. 7. Phase portrait slightly below the point *e* near the fixed point *A* and the corresponding pursuit graph at point *e* in global coordinates

bifurcations on the stability boundary. Both analytical and numerical results (not provided here) show that the communication has no qualitative effect on the final consensus dynamics of the agent collective. As briefly stated in section I, the future research direction includes the more generalized nonlinear dynamic analysis of two unicycles, not necessarily in leader-follower configuration and extending the result for multiple unicycles with communication delay.

REFERENCES

[1] J. K. Parrish, S. V. Viscido, and D. Grünbaum, Self-organized Fish Schools: An Examination of Emergent Properties. *Biol. Bull.*, 202: 296-305, 2002.

[2] H.-S., Niwa, Newtonian Dynamical Approach to Fish Schooling. *Journal of Theoretical Biology*, 181: 47-63, 1996.

[3] S. Gueron, S. A. Levin, and D. I. Rubenstein, The Dynamics of Herds: From Individuals to Aggregations. *Journal of Theoretical Biology*, 182: 85-98, 1996.

[4] C. W. Reynolds, Flocks, Herds and Schools: A Distributed Behavioral Model. *Computer Graphics*, 21 (4): 25-34, 1987.

[5] C. R. McInnes, Distributed Control for On-orbit Assembly. *Advances in the Astronautical Sciences*, 90: 2079-2092, 1996.

[6] E. Justh, and P. Krishnaprasad, A Simple Control Law for UAV Formation Flying. Technical Report, TR 2002-38, Institute for Systems Research, University of Maryland, 2002.

[7] Y. Cao, W. Ren, N. Sorensen, L. Ballard, A. Reiter, and J. Kennedy, Experiments in Consensus-based Distributed Cooperative Control of Multiple Mobile Robots. *Proc. of the 2007 IEEE International Conference on Mechatronics and Automation*, 2819-2824, 2007.

[8] D. Helbing, I. Farkas, and T. Vicsek, Simulating Dynamical Features of Escape Panic. *Nature*, 407: 487-490, 2000.

[9] L. Fang, and P. J. Antsaklis, On Communication Requirements for Multi-agent Consensus Seeking. *LNCS*, 331: 53-67, 2006.

[10] D. V. Dimarogonas, and K. J. Kyriakopoulos, On the State Agreement Problem for Unicycles. *Proc. of the 2006 American Control Conference*, 2016-2021, 2006.

[11] J. Lin, A. S. Morse, and B. D. O. Anderson, The Multi-agent Rendezvous Problem. *Proc. of the 42nd 2003 IEEE Conference on Decision and Control*, 1508-1513, 2003.

[12] R. Olfati-Saber, and R. M. Murray, Consensus Problems in Networks of Agents with Switching Topology and Time-delays. *IEEE Transactions on Automatic Control*, 49 (9): 1520-1533, 2004.

[13] A. Bernhart, Polygons of Pursuit. *Scripta Mathematica*, 24: 23-50, 1959.

[14] J. A. Marshall, M. E. Broucke, and B. A. Francis, Formations of Vehicles in Cyclic Pursuit. *IEEE Transactions on Automatic Control*, 49 (11): 1963-1974, 2004.

[15] J. A. Marshall, M. E. Broucke, and B. A. Francis, Pursuit Formations of Unicycles. *Automatica*, 42 (1): 3-12, 2006.

[16] J. P. Desai, J. P. Ostrowski, and V. Kumar, Modeling and Control of Formations of Nonholonomic Mobile Robots. *IEEE Transactions on Robotics and Automation*, 17 (6): 905-908, 2001.

[17] A. K. Das, R. Fierro, V. Kumar, J. P. Ostrowski, J. Spletzer, and C. J. Taylor, A Vision-based Formation Control Framework. *IEEE Transactions on Robotics and Automation*, 18 (5): 813-825, 2002.

[18] A. Jadbabaie, J. Lin, and A. S. Morse, Coordination of Groups of Mobile Autonomous Agents using Nearest Neighbor Rules. *IEEE Transactions on Automatic Control*, 48 (6): 988-1001, 2003.

[19] P. Yang, R. A. Freeman, and K. M. Lynch, Multi-agent Coordination by Decentralized Estimation and Control, To appear, *IEEE Transactions on Automatic Control*, 2008.

[20] R. A. Freeman, P. Yang, and K. M. Lynch, Distributed Estimation and Control of Swarm Formation Statistics. *2006 American Control Conference*, Minneapolis, Minnesota, 749-755, June 2006.

[21] J. Lin, A. S. Morse, and B. D. O. Anderson, The Multi-agent Rendezvous Problem Part 2: The Asynchronous Case. *SIAM Journal on Control and Optimization*, 46 (6): 2120-2147, 2007.

[22] L. Fang, P. J. Antsaklis, and A. Tzimas, Asynchronous Consensus Protocols: Preliminary Results, Simulations and Open Questions. *Proc. of the 44th 2005 IEEE Conference on Decision and Control*, 2194-2199, 2005.

[23] Y. Liu, K. M. Passino, and M. Polycarpou, Stability Analysis of One-dimensional Asynchronous Swarms, *IEEE Transactions on Automatic Control*, 48(10): 1848-1854, 2003.

[24] V. Gazi, Stability of an Asynchronous Swarm with Time-dependent Communication Links, *IEEE Transactions on Systems, Man and Cybernetics, Part B: Cybernetics*, 38(1): 267-274, 2008.

[25] D. Hristu-Varsakelis and C. Shao, A Bio-Inspired Pursuit Strategy for Optimal Control with Partially-Constrained Final State, *Automatica*, 43(7): 1265-1273, 2007.

[26] M. G. Earl, and S. H. Strogatz, Synchronization in Oscillator Networks with Delayed Coupling: A Stability Criterion. *Physical Review E*. 67 (3): 036204.1-036204.4, 2003.

[27] S. Zhao, and T. Kalmár-Nagy, Nonlinear Dynamics of Uni-cyclic Pursuit. *2008 IEEE Multi-Conference on Systems and Control*, 3-5 Sep. 2008, San Antonio, Texas, USA.

[28] N. J. Mathai, and T. Zourntos, Emergent Fluctuations in the Trajectories of Agent Collectives. *Fluctuations and Noise Letters*, 7 (4): L429-L437, 2007.

[29] D. Hammel, Formation Flight as an Energy Saving Mechanism. *Israel Journal of Zoology*, 41: 261-278, 1995.

[30] M. Andersson, and J. Wallander, Kin Selection and Reciprocity in Flight Formation. *Behavioral Ecology*, 15 (1): 158-162, 2004.

[31] W. S. Levine, Control System Fundamentals. *CRC Press*, 2000.

[32] Y.A. Kuznetsov, Elements of Applied Bifurcation Theory. *Springer*, 2004.

[33] J. Guckenheimer, and P. Holmes, Nonlinear Oscillations, Dynamical Systems, and Bifurcations of Vector Fields. *Springer*, 1983.